DOI: 10.21120/LE/18/2/4

*Acta Geographica Debrecina*
*Landscape & Environment series 18 (2) 2024. 43-62*

# URBANIZATION INDUCED LAND USE/LAND COVER CHANGE AND ITS IMPACT ON LAND SURFACE TEMPERATURE IN BHUBANESHWAR CITY, INDIA

**MADHUSMITA PARIDA[1], GARIMA JASROTIA[1], KIRAN KUMARI SINGH[2]***

1Department of Geography, Central University of Punjab, Bathinda, India
2 Department of Geography, University of Allahabad, Prayagraj, India
*Email: ksingh@allduniv.ac.in

Received 24 February 2024, accepted in revised form 13 May 2024



**Abstract**
Land transformation and increasing heat are some of the challenges cities are grappling with. This study investigated the impact of land transformation on surface temperature by retrieving land surface temperature (LST), normalized difference vegetation index (NDVI), and normalized difference built-up index (NDBI) in Bhubaneswar city, India. The study employed Landsat 5 data for the years 2001 and 2011 and Landsat 8 data for the year 2021. The surface urban heat island (SUHI) effect was further studied to identify temperature changes and hotspots in the city. The heating effect of built-up and cooling effect of vegetation was ascertained through correlation analysis between LST and NDBI (positive) and LST and NDVI (negative). The result of this study indicates significant land cover transformation in Bhubaneswar city with expansion in built-up area from 19.05 sq km to 46.98 sq km between 2001 to 2021. During the same period, the maximum value of LST increased by 3.93°C and the minimum value of LST increased by 1.55°C in the city. This study emphasizes the need for strategic urban planning by underscoring the impact of land cover transformation on LST. Identification of heat stressed areas is important to prepare action plans to mitigate the heat impact as India strives to create sustainable and smart cities.

***Keywords:*** Land Surface Temperature (LST); NDBI; NDVI; Urban hot spots; Bhubaneshwar

## 1. Introduction

Urbanisation severely affects the world and causes unusual changes in climate patterns. It leads to substantial land use changes in the city region by construction of different infrastructures for habitation, transportation, industry, and other reasons. The infrastructures of growing cities expand quickly, transforming natural ground surfaces into impermeable, built-up areas. Simple rural structures are replaced with composite urban structures and extensive industrial and commercial activities take over agricultural operations. The result is a massive conversion of land, previously occupied by vegetation cover and soil, into concrete and asphalt surfaces. Compared to natural ground surfaces, asphalt, concrete, and brick absorb more solar energy, thereby, raising surface and air temperatures (Sharma et al. 2021). As a result, urbanisation significantly impacts Land Surface Temperature (LST) by disrupting the surface energy balance (Das et al. 2022). LST refers to 'how hot the Earth's 'surface' feels to touch' in a certain region. It is

different from air temperature shown in the daily weather reports (Mathew et al. 2016). For a satellite, the 'surface' is whatever it sees when looking down through the atmosphere to the ground. It can be snow and ice, grass on a lawn, roof of a building, or leaves in the canopy of a forest (Li and Duan 2017). Thus, LST is a direct measure of the temperature of the earth's surface, which varies according to geological, geophysical, and geochemical factors of the ground. It is one of the most important aspects of climate change. The warmth rising off the Earth's landscapes influences our world's weather and climate patterns, making it important to keep track of the LST.

LST is also responsible for changing micro-climate of an area and creating the Urban Heat Island (UHI) effect (Al-Ruzouq et al. 2022). The higher LST of urban impervious surfaces compared to peripheral rural areas creates a sharp temperature gradient to the extent that urban areas become significantly hotter than their surroundings. This is what is referred to as the UHI effect, also known as 'urban heat sink' or the 'oasis' effect (Anasuya et al. 2019; Derdouri et al. 2021; Shahfahad et al. 2022). In simpler words, UHI is a phenomenon in which urban areas experience higher temperatures than their surrounding rural areas (Najafzadeh et al. 2021). UHIs are further classified into two broad categories namely, Surface UHI (SUHI) and Atmospheric UHI (AUHI)- the main differences between the two being the way they are formed and the different methods used to study them. AUHI has its origin in the difference in air temperature in and around a region and is usually measured from ground-based stations and field surveys. SUHI, on the other hand, results from the type and temperature of the ground surface and is mainly studied using satellite data (Derdouri et al. 2021; Wang et al. 2016). The rise in LST of an area may be due to several reasons like burning of fossil fuels, emissions from vehicles, deforestation, increase in urban population, increase in urban infrastructure, etc. The clustering of a few or all of these factors lead to an uneven increase of temperature within the already existing UHI and creates urban hot spots. The opposite is true in patches of dense green-blue spaces where cooling effect is associated with vegetation and water, leading to the formation of urban cold spots (Shahfahad et al. 2022). High LST and its effects on the micro climate of an area not only lead to heat stress but also to extreme weather events, often resulting in rapid and high precipitation and flash floods during the rainy season. In fact, an 'urban rain island', such as in Jinan city, China, is a resultant phenomenon of UHI (Derdouri et al. 2021). The vulnerability of any city to such events makes its inhabitants, particularly the poor, vulnerable to problems ranging from mild discomfort to serious health issues resulting in death (Alves et al. 2020). Broadly speaking, UHI and its associated phenomena are a major barrier to achieving the targets set by sustainable development goals (SDGs), particularly SDG 11 and 13 (Derdouri et al. 2021). Since the study of UHI and hot or cold spots depends on study of LST, it becomes necessary to understand and analyse the relationship among LST, LULC change, and UHI effect to better plan and manage urban areas. This is imperative in mitigating the critical effects of increased LST and UHI on cities and their dwellers (Alves et al. 2020).

Since the 1990s, a number of works have been carried out to assess the LULC change dynamics and their impacts on LST in Bhubaneshwar city. Their results collectively indicate a decline in vegetation cover due to an increase in built up, an increase in mean LST of the city, the seasonality of LST, NDVI, SUHI, and differences in the distributional pattern of LST in the city (core-periphery, scattered-concentrated, direction of high LST etc). These works have established statistically significant correlations of LST with NDBI (positive), NDVI and NDWI (negative) etc. (Das et al. 2022; Sarkar 2022), emphasising that the increase in built up leads to a decrease in vegetation and crop cover and an increase in the mean LST in Bhubaneswar city. For example, the built-up

area in Bhubaneswar increased by 77% from 2003-2008 (Anasuya et al. 2019) and 70% from 2000-2020 (Garg 2022). At the same time, a decline of 89% and 83% in dense vegetation and croplands respectively from 2000-2014 (Swain et al. 2017) and a total reduction of 26.47 km2 vegetation cover from 2001-2021 (Samal et al. 2022) were observed. The LST increased by an average of approximately 4˚C to 6 ˚C between 2001 and 2021 (Garg 2022; Samal et al. 2022). The pattern of temperature distribution over the city also changed from scattered to concentrated (1997-2017) (Sarkar 2022), with the mean LST over 'pervious' spaces being higher than their surroundings (Anasuya et al. 2019). For SUHI extraction, both the 'LST as a proxy' (Kumar 2019) and 'buffer creation' methods were used (Sethi et al. 2022; Chaudhuri 2020). The works pertaining to UHI effect are far and few but clearly indicate an increase in UHI values over the periods of their study (Tah Mukherjee, 2022; Nandini et al. 2022; Chaudhuri, 2020). Despite the work done on LST, UHI and urban hotspots (Magotra et al. 2020; Garg 2023), till now, a comprehensive study covering the dynamics of SUHI, hot spots and cold spots of Bhubaneswar city is missing. The main aim of this study is to reduce this gap. The detailed objectives, here, are (a) to study spatial patterns of Land Surface Temperature (LST), Normalized Difference Vegetation Index (NDVI), and Normalized Difference Built-up Index (NDBI) in Bhubaneshwar city for the years 2001, 2011 and 2021; (b) to establish the relationship between LST and spectral indices – NDVI and NDBI across Bhubaneswar city; (c) to explore the presence of urban hotspots (UHS) in Bhubaneswar city based on retrieved LST values; and (d) to derive Surface Urban Heat Island (SUHI) and analyse the impact of urban greenness, water bodies, barren, and built-up on LST over these two decades.

## 2. Materials and methods

### Area of study

The area of interest for this study is Bhubaneswar Municipal Corporation (BMC) (Fig. 1), hereby referred to as Bhubaneswar city. It is the capital and the largest city of Odisha, an east Indian state flanked by Jharkhand in the north, Andhra Pradesh in the south, Bay of Bengal in the east, and Chhattisgarh in the west. The city is located in Khordha district of Odisha, on the banks of Kuakhai and Daya rivers in the Mahanadi River basin. Falling between 20o12'N- 20 o25'N latitudes and 85o 44'E- 85 o55'E longitudes, it spans over an area of 146.60 sq. km (Bhubaneswar Development Authority, n.d.). The city has a humid and tropical climate with the average annual temperatures of 32 °C (maximum) and 27 °C (minimum) and the average annual precipitation of 1542 mm ("City Development Plan Report" 2014; Magotra et al. 2020). The soil is hard red laterite in the northern and western parts and fertile alluvial in the eastern and southern parts resulting in mixed (moist deciduous) vegetation (Pritipadmaja and Garg, 2022). It is one of the first planned cities of modern India and has a population size of 8,85,363 inhabitants (Census of India, 2011). Bhubaneswar is a centre of heritage tourism, trade and commerce, and occupies the central position in the 'Golden Triangle' of the east between Puri and Konark (City Development Plan Report, 2014).

Contrary to the urbanisation experience of the state of Odisha (one of the least urban states of India with 16.65% of its population being urban), its capital has witnessed rapid urbanisation leading to an accelerated growth of not only population and built-up but also of the economy (Census of India, 2011; Magotra et al. 2020). This growth has resulted in large scale conversion of vegetation and fallow

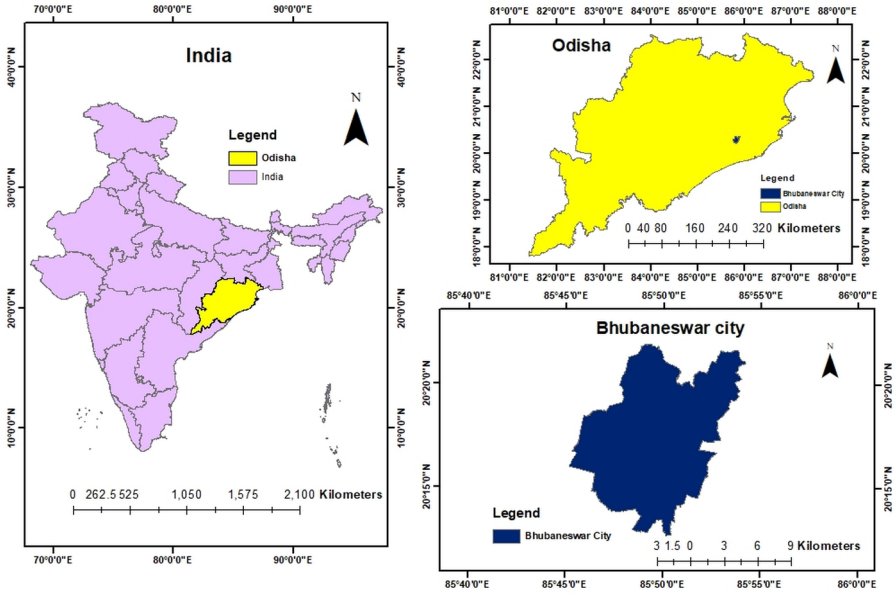


Fig. 1. Study area

land into urban infrastructure. This increased urban structures (increase of~83%) have added to heat stress ( Das et al. 2022). Not only have the number of days with severe heat waves been steadily increasing but a recent trend of rise in the land surface temperature (0.25 °C/year) is also observed (Sethi et al. 2022). All this makes it imperative to study the changes in land cover and resultant impacts on temperature of the city surface.

The FCC map (Fig. 2) of Bhubaneswar gives an idea of the land cover of the city in three different years. Here, the red colour shows vegetation (denser the vegetation, darker the colour), dark blue and black colour show water bodies, the bright colour (white) shows the vacant land, slightly greenish colour shows the barren and fallow land, and silver colour shows the urban area.

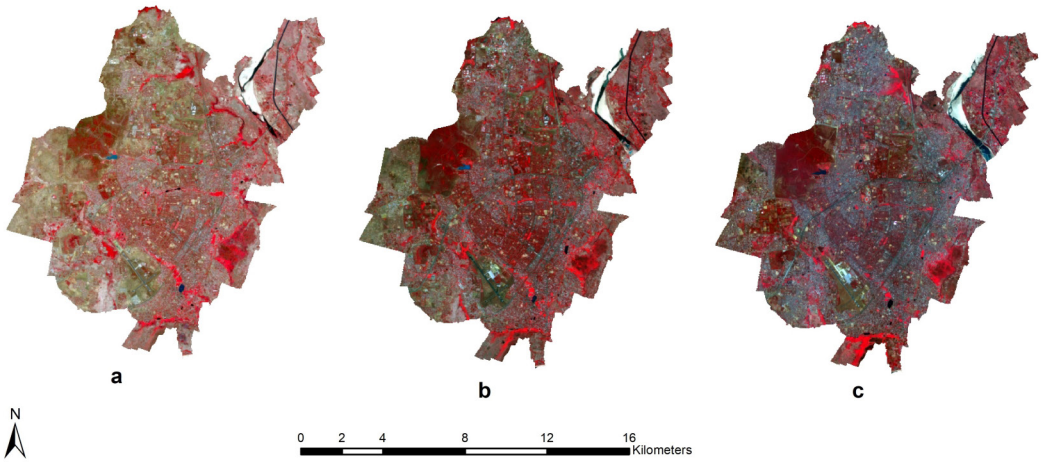


Fig. 2. False Colour Composition images of Bhubaneswar city for the years: a) 2001; b) 2011; c) 2021

### *Data acquisition and analysis*

Ever since access to satellite data became commonplace, especially with the launch of Landsat series in 1972, remote sensing and GIS have been used to study the spatio-temporal changes in urban temperature and climate (Derdouri et al. 2021). For this study, Landsat 5 Thematic Mapper (TM) for 2001 and 2011 and Landsat 8 Operational Land Imager and Thermal Infrared Sensor (OLI/TIRS) for 2021 were acquired from United States Geological Survey (USGS) earth explorer database. These imageries of 30m resolution were of pre-monsoon period (March-April). This period of acquisition was selected in order to minimize cloud cover and seasonal variations in green and blue spaces i.e. to provide uniformity for better differentiation between built-up and other classes, and a relatively easier analysis of LST (Anasuya et al. 2019; Dibaba 2023). Thermal bands were used for LST calculation whereas optical bands were used for NDBI and NDVI calculation. Atmospheric correction of the bands was done using QGIS 3.16 software and LST, NDBI, and NDVI were calculated using ArcGIS 10.8 software. Table 1 provides a detailed account of the datasets used.

### *Derivation of Land Surface Temperature*

Band 6 of Landsat 5 TM and band 10 of Landsat 8 OLI/TIRS were used to extract the LST data as only thermal bands are needed for extracting land surface temperature. A total of four main steps were followed to arrive at final LST values from the initial digital numbers (DN) of pixels. The first step was to extract Spectral Radiance from pixels of satellite data. Since this involves different methods of calculation for Landsat 5 and 8, (Eq. 1) was used for Landsat 5 (Dibaba 2023) and (Eq. 2) for Landsat 8 imagery ("Landsat 8 Data Users Handbook n.d"). For the remaining steps, same formulae were followed for both datasets.

#### *Step 1: Generating Spectral Radiance ($L_\lambda$) values from DN*

Spectral Radiance is the amount of energy radiated across different wavelengths, including visible and thermal, that is recorded by a satellite sensor (Mathew et al. n.d.).

For Landsat 5 TM, it was calculated using (Dibaba 2023) the given equation:

$$L_\lambda = [(LMAX_\lambda - LMIN_\lambda) / (QCALMAX - QCALMIN)] * (QCAL - QCALMIN) + LMIN_\lambda \quad (1)$$

Where,

QCAL – DN value of pixel

QCALMAX – Maximum DN value of pixel i.e. 255

QCALMIN - Minimum DN value of pixel i.e. 1

$LMAX_\lambda$ - Maximum spectral radiance scaled to QCALMAX

$LMIN_\lambda$ - Minimum spectral radiance scaled to QCALMIN

Table 1: Details of datasets

| Data Type | Sensor | Acquisition date | Band used for LST derivation (Resolution) | Band used for NDVI derivation (Resolution) | Band used for NDBI derivation (Resolution) |
|---|---|---|---|---|---|
| Landsat 5 | TM | 15 March 2001 | Band 6 (120 m) | Band 3 & 4 (30 m) | Band 4 & 5 (30 m) |
| Landsat 5 | TM | 12 April 2011 | Band 6 (120 m) | Band 3 & 4 (30 m) | Band 4 & 5 (30 m) |
| Landsat 8 | OLI/TIRS | 6 March 2021 | Band 10 (100 m) | Band 4 & 5 (30 m) | Band 5 & 6 (30 m) |

For Landsat 8 OLI/TIRS, the following formula (Landsat 8 Data Users Handbook. n.d.) was used to convert DN to spectral radiance:

$$L_\lambda = (M_L)*(DN)+A_L \quad (2)$$

Where,

$M_L$- Radiance Multiband

$A_L$- Radiance add band

DN - Digital number of the pixel

The $M_L$ and $A_L$ values were obtained from the metadata of respective satellite data.

*Step 2: Generating Brightness Temperature (T) values using Spectral Radiance ($L_\lambda$)*

Brightness temperature (T) is essentially the way to measure the temperature of an object that is derived by measuring the intensity of electromagnetic energy radiated by it (Mathew et al. n.d.).

The $L_\lambda$ values obtained in Step 1 were used to calculate the brightness temperature (T), which is the real or effective temperature recorded by the satellite under the pre-condition that the value of emissivity is one (Landsat 8 Data Users Handbook n.d.; Wang et al. 2015), using the following (Eq. 3) formula:

$$T = K_2 / \ln (K_1/L_\lambda + 1) - 273.15 \quad (3)$$

Where,

$k_1$- Calibration constant 1

$K_2$ - Calibration constant 2

Values of $k_1$ and $K_2$ were acquired from the satellite metadata (table 2) and absolute zero (approx. - 273.15 ◦ C) was added to the formula to get results in degree Celsius.

*Step 3: Generating Land surface emissivity (ε) values*

The emissivity of land surface depends upon different aspects namely its composition, structure, roughness etc. Since the value of T is derived using emissivity value of a black body i.e. 1, it becomes necessary to correct the spectral emissivity based on the land cover type under observation.

Here, the spectral emissivity (ε) correction was done on the basis of NDVI values using the formula (Eq. 4) given below:

$$\varepsilon = 0.004*P_v +0.986 \quad (4)$$

Where,

Pv - Proportion of vegetation derived from NDVI using (Eq. 5)

$$Pv = \text{Square}((NDVI - NDVI_{min}) / (NDVI_{max} - NDVI_{min})) \quad (5)$$

The minimum and maximum values of NDVI mentioned above were obtained after the derivation of NDVI indices (Eq. 7).

*Step 4: Generating Land surface temperature (LST) values*

The LST was calculated using corrected emissivity values with the following (Deoli, 2020) formula (Eq. 6):

$$LST = (T / (1 + (0.00115 * T / 1.4388) * \ln(\varepsilon))) \quad (6)$$

***Spectral Indices***

The Spectral indices namely NDVI and NDBI were calculated to assess the impact of land use and land cover change on LST by using their results as proxy of LULC classes, particularly for identification of healthy dense vegetation and impervious built-up areas.

*Normalized Difference Vegetation Index (NDVI)*

NDVI is a numerical indicator used to monitor the quantity, quality, and changes in vegetation characteristics of a region. It is calculated using the ratio of red (R) and

Table 2. Value table for Landsat 5 and Landsat 8

| Calibration constant | Landsat 5 | Landsat 8 |
|---|---|---|
| K1 | 607.76 | 774.8853 |
| K2 | 1260.56 | 1321.0789 |

Source: Authors (Adapted from Das et al. 2022)

near-infrared (NIR) spectral bands. The NDVI values range between +1.0 and -1.0. The negative values denote water bodies and the near 0 values indicate barren land (Halder et al. 2022).

For Landsat 5 data, bands 3 and 4 and for Landsat 8 data, bands 4 and 5 were used to calculate NDVI using the formula below (Eq. 7).

$$NDVI = NIR - R / NIR + R \quad (7)$$

*Normalized Difference Built-up Index (NDBI)*

NDBI is used to monitor built-up area using the ratio of short-wave infrared (SWIR) and near-infrared (NIR) spectral bands. The NDBI values range between +1.0 and -1.0 with positive values denoting built up, negative denoting water body, and near zero denoting vegetation (Halder et al. 2022).

For Landsat 5 data, bands 5 and 4 and for Landsat 8 data, band 6 and 5 were used to calculate NDBI using the following formula (Eq. 8).

$$NDBI = SWIR - NIR / SWIR + NIR \quad (8)$$

### *Derivation of Surface Urban Heat Island (SUHI)*

The SUHI is a type of UHI that is considered an important tool to monitor heat and thermal balance of an urban land surface. For this study, it is calculated using the buffer zoning method which involves finding the difference of temperature intensity between the core and buffer area (Li et al. 2013).

The following (Eq. 9) formula (Alves et al. 2020) was used for its derivation:

$$SUHI = BTU - BTR \quad (9)$$

Where,

$BT_U$ - Surface temperature of each urban pixel

$BT_R$ - Average surface temperature of buffer zone (rural) created around the urban boundary.

### *Delineation and Analysis of Urban Hot Spots (UHS)*

Urban hot spots are small areas within the urban heat islands with significantly higher temperatures than their surroundings (Abir et al. 2021). In this study, UHS have been delineated using two different methods.

*Percentile Method*

The following method (Eq. 10) shows small hotspot patches in the map using LST > μ at 95% confidence interval.

$$LST > \mu + 2*\sigma \quad (10)$$

Where,

μ – Mean LST ( ◦ C)

σ - Standard deviation LST

*Getis-Ord Gi* tool*

The hot spots were identified using Getis-Ord Gi* tool in ArcGIS 10.8 software. Also known as cluster analysis, it is a statistical tool based on spatial autocorrelation model that identifies statistically significant geographic hotspots of high and low values. It works by looking at each feature within the context of the neighbouring features (Halder et al. 2022; Jana ¬– Sar, 2016). The resultant z score and p values identify areas having high or low values of spatial clustering. The high positive z score and small p value indicate intense clustering of high values (hot spot) whereas negative z score and small p value indicate more intense clustering of low values (cold spot). A near zero value indicates no obvious spatial clustering (Jana – Sar 2016). Before using this tool, the LST values were extracted through 1350 points with the help of the "Fishnet tool" in ArcGIS using which the significant clustering of hotspots and cold spots were visualised.

### *Correlation analysis*

For the current study, the correlation analysis between LST and NDVI as well as LST and NDBI was done using Pearson's coefficient of correlation method. This was done to show the level of association and

dependence amongst these variables (Turney 2022). A linear regression (R2) analysis using scatter plots was also conducted using data analysis tool of Excel for determining the predictability of dependent variable (y) from independent variable (x). The R2 vales range from 0 to 1 wherein the extent of predictability increases as its value moves from 0 (i.e. 0%) to 1 (i.e. 100%) (Frost n.d.; Vadapalli 2023).

## 3. Results and Discussion

### Spatio-temporal patterns of NDBI, NDVI, and LST

#### *NDBI*

The classification of non-built-up, built-up, and barren has been done by manual thresholding. From figure 3, it is clear that the built-up area (red) has increased significantly whereas the barren land (yellow) has decreased from 2001 to 2021.

Table 3 shows the threshold values taken to derive built-up area and baren area through manual thresholding process. Analysis of NDBI values (Table 3) shows that the built-up area has increased from 19.05 sq. km to 36.10 sq. km between 2001 and 2011 and from 36.10 sq. km to 46.98 sq. km in 2021 i.e. a total increase of 27.93 sq. km in two decades. Here, a unique observation is the higher value of NDBI in 2001 due to the availability of more barren land in 2001 compared to more vegetation in 2011. However, there is a visible decline in vegetation in 2021, particularly in the central part of the city, which is replaced by built up.

#### *NDVI*

A higher value of NDVI represents dense greenery. Generally, the values from -1 to 0 represent water bodies, -0.1 to 0.1 represent

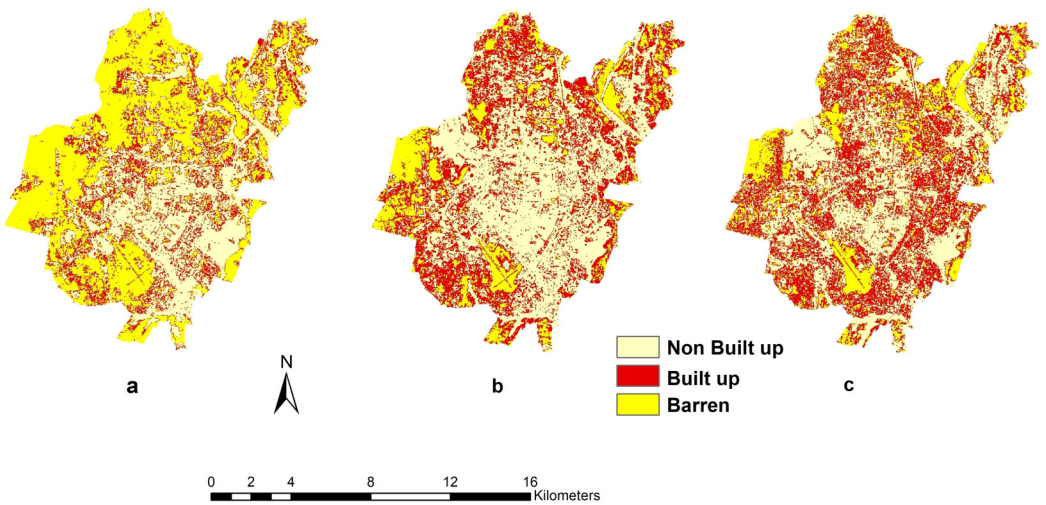


Fig. 3. Map showing change in built up area of year: a) 2001; b) 2011: c) 2021

Table 3: NDBI threshold values

| Class | 2001 | | 2011 | | 2021 | |
|---|---|---|---|---|---|---|
| | Min | Max | Min | Max | Min | Max |
| Non-Built up | -0.42 | 0.12 | -0.44 | 0 | -0.46 | 0.09 |
| Built up | 0.12 | 0.18 | 0 | 0.08 | 0.09 | 0.16 |
| Barren | 0.18 | 0.39 | 0.08 | 0.29 | 0.16 | 0.44 |

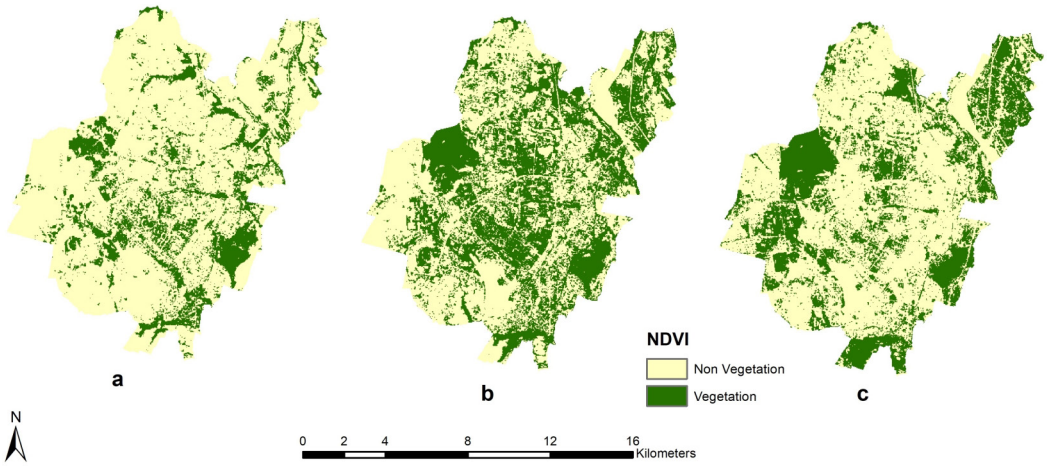


Fig. 4. Map showing changes in vegetation in the year: a) 2001; b) 2011: c) 2021

Table 4: NDVI threshold values

| Class | 2001 | | 2011 | | 2021 | |
|---|---|---|---|---|---|---|
| | Min | Max | Min | Max | Min | Max |
| Vegetation | 0.43 | 0.85 | 0.25 | 0.63 | 0.40 | 0.83 |
| Non-vegetation | -0.22 | 0.43 | -0.15 | 0.25 | -0.18 | 0.40 |

barren rocks, 0.2 to 0.5 represent shrubs and grasslands, and 0.6 to 1.0 represent dense vegetation (Kshetri 2018). The binary image (Fig. 4) of vegetation and non-vegetation classes is created by manual thresholding using the threshold values given in table 4. Vegetation patches have increased in the north central part of the city i.e., in the area of educational institutes (Institute of Minerals and Materials Technology, Institute of Physics, Utkal University) near Sachivjaya marg.

The area under vegetation cover was 30.75 sq. km, 63.59 sq. km, and 50.25 sq. km in 2001, 2011, and 2021 respectively. Despite a decline in vegetation cover from 2011 to 2021, an overall increase of 19.5 sq. km is observed from 2001 to 2021. The increase is concentrated in the western, southern, and northern parts of the city and the central part saw a declining share of vegetation in 2021.

### *Land Surface Temperature (LST)*

The highest LST values (Fig. 5) for 2001, 2011, and 2021 are 35.25 ℃, 39.16 ℃, and 39.18 ℃ respectively and the lowest LST values for 2001, 2011, and 2021 are 24. 97℃, 26.25℃, and 26. 46℃ respectively. Thus, from 2001 to 2011 the rise in maximum LST is 3.91 ℃ and from 2011 to 2021, it is 0.006 ℃ i.e. a significant increase of 3.93℃ in two decades. The minimum temperature has also risen by 1.55℃ during the same period.

A major part of the city experienced temperatures between 32 ℃ and 39 ℃ in 2021 compared to 2001 (Fig. 6) when very small patches of 34 ℃ to 36 ℃ range were seen at the airport, sand beds, and vacant lands. The spatial distribution of LST has also changed in the last two decades. In 2001, high LST was observed in scattered patches in the north and south of the city due to the presence of vacant area. In 2011, the south-western, western, and north-eastern parts were hotter while in 2021, these hotter patches have expanded more (the airport, sand bed region in north, vacant land in west, and residential zone and industries-Mancheswar in north eastern part of the city) (Fig. 7). The pattern is opposite in case of low LST patches like water bodies

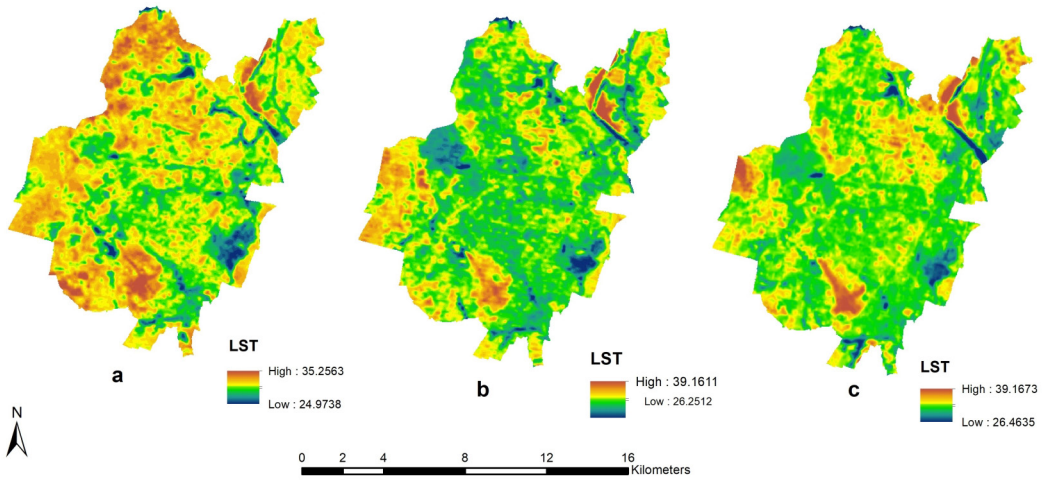


Fig. 5. Land Surface Temperature in (°C) in year: a)2001; b)2011; c)2021

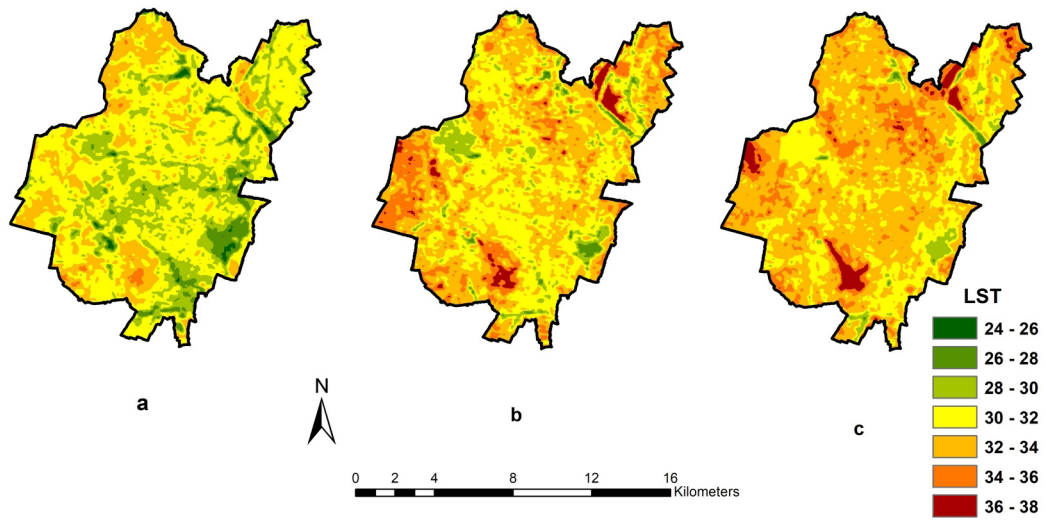


Fig. 6. Classified Land Surface Temperature in (°C) in year: a) 2001; b)2011; c) 2021

(Bindu Sagar, Ekamra Kanan lake, Kuakhai river) and vegetation (Bharatpur Forest, Jaydev Bhatika, Near railway track in the northern part of city). Despite a higher green cover in 2011 compared to 2001, not only the surface temperature of the sand bed region and vacant land was higher but also that of the greener central part of the city. In 2001, the LST of the central part of the city was between 28 °C to 30 °C while it rose to 30°C to 32°C in 2011, and 32°C to 34°C in 2021.

Figure 7 shows LST profile line graphs of different land features drawn upon the LST map of the city for the year 2021. Here, the vertical axis shows the LST and the horizontal axis shows the land features. The profile line from A to B in the southern part of the city is drawn by crossing it over the airport region, from C to D in the western part over vacant land and forest, and from E to F in the northern part over the sand bed region of the city. Line A to B passes through a waterbody (28 °C), built up (34 °C in the settlement area and 36°C in the airport region), and vegetation (33 °C). Line C to D passes through fallow land (38 °C), vegetation (31 °C), and a

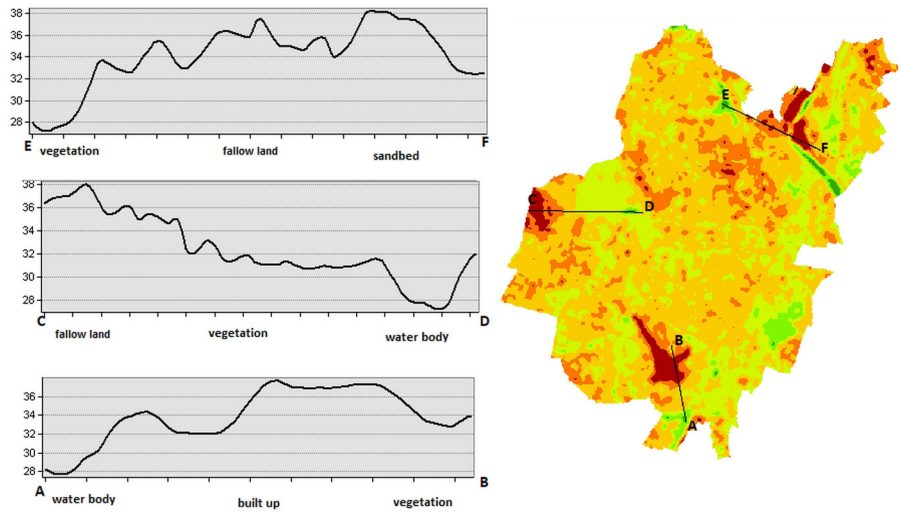


Fig. 7. Showing temperature of different features in profile graph

Table 4: Statistical characteristics of LST, NDVI and NDBI

| | 2001 | | | | 2011 | | | | 2021 | | | |
|---|---|---|---|---|---|---|---|---|---|---|---|---|
| | Min | Max | Mean | SD | Min | Max | Mean | SD | Min | Max | Mean | SD |
| NDVI | -0.22 | 0.85 | 0.35 | 0.1 | -0.15 | 0.63 | 0.24 | 0.08 | -0.18 | 0.83 | 0.37 | 0.1 |
| NDBI | -0.42 | 0.39 | 0.14 | 0.11 | -0.44 | 0.29 | -0.01 | 0.09 | -0.46 | 0.44 | 0.08 | 0.09 |
| LST | 24.97 | 35.25 | 30.56 | 1.51 | 26.25 | 39.16 | 32.18 | 1.75 | 26.46 | 39.17 | 32.78 | 1.49 |

water body (26 °C). Line E to F passes through vegetation (26 °C), fellow land (37 °C), and the sand bed region (39 °C) of the city.

The minimum, maximum, mean, and standard deviation values of NDVI, NDBI, and LST for the years 2001, 2011, and 2021 are given below (Table 5).

## Relationship between LST & NDVI and LST & NDBI

To examine the patterns of relationship between LST and the two spectral indices - NDVI and NDBI, respectively, several points from the LST images were chosen as samples and the NDVI and NDBI values were retrieved for the same sample locations. Some points were manually removed because the NDVI points falling in water body showed negative values and lower LST.

Table 6 shows a positive correlation between LST and NDBI but a negative correlation between LST and NDVI. This means that an increase in urban built-up spaces leads to an equivalent rise in LST whereas an increase in green spaces leads to lowering of LST in surrounding areas. Albeit having a strong positive correlation between LST and NDBI in all three years of study, a stronger positive value is seen in 2001 and 2011 compared to 2021 despite an

Table 4: Statistical characteristics of LST, NDVI and NDBI

| Year | NDVI | NDBI |
|---|---|---|
| 2001 | -0.6546 | 0.780607 |
| 2011 | -0.57801 | 0.743682 |
| 2021 | -0.3658 | 0.683479 |

increase in built-up area from 2001 to 2021. This may be attributed to a higher number of vacant land patches in 2001. However, in case of NDVI and LST, there is a decline in the relationship strength from strong negative in 2001 to moderate in 2011 and weak in 2021 (McSeveny et al. 2014). Figures 8 and 9 show the distribution of LST, NDVI, and NDBI values over 2001, 2011, and 2021 as well as the coefficient of determination (R2) values. These are high for NDBI (0.6093, 0.8498, and 0.8666 for 2001, 2011, and 2021 respectively) but low for NDVI (0.4285, 0.3341, and 0.1338 for 2001, 2011, and 2021 respectively) indicating not only lower dependence of LST on NDVI but also a decline in the dependency with every passing decade.

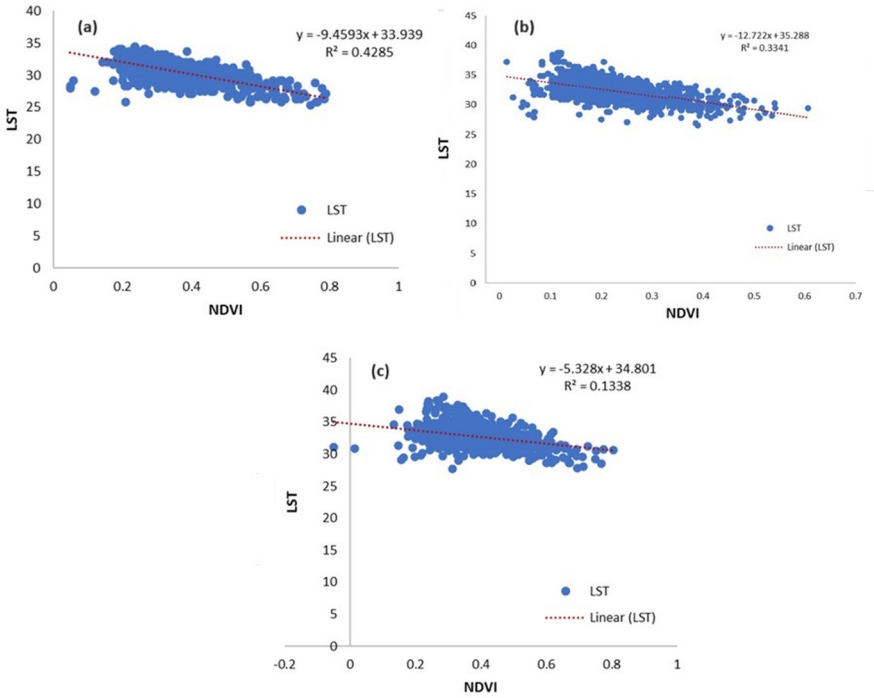


Fig. 8. LST and NDVI: a) 2001; b) 2011; c) 2021

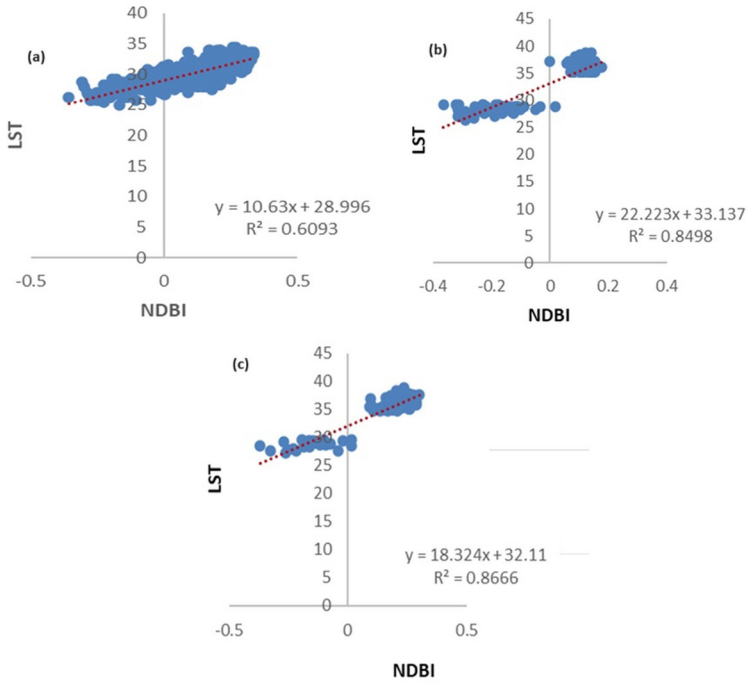


Fig. 9. LST and NDBI: a) 2001; b) 2011; c)2021

## Hotspot analysis

### *Getis-Ord Gi* tool*

The map below (Fig. 10) shows the hot and cold spots of the city using the Getis-Ord Gi* tool. The hotspots represent the clusters of points having high LST and the cold spots represent the clusters of points having low LST. In figure 10 a (2001), the LST hotspots are located in the northern part of the city and the airport whereas the cold spots are located in the south-eastern part of the city covered with vegetation. In 2011 (Fig. 10 b), the hotspots seem to have expanded to the south eastern part of the city and the sand bed region whereas the cold spots are present in the western and eastern parts of the city and other areas under vegetation cover. In 2021 (Fig. 10 c), the hotspots patches have further increased to include vacant land and sand bed of the city. Moreover, the hotspots with 95% confidence are covering the north-eastern part of the city (residential zone as well as industrial zone of BMC) whereas the cold spots (90% and above confidence) are in the eastern part of the city and in the Kuakhai river. The hot spots with 99 % confidence have a higher presence in 2021 compared to 2001 and 2011.

### *Surface Urban Heat Island (SUHI)*

The urban heat island effect is mainly caused by anthropogenic changes to the natural earth surface. It leads to rise in surface and air temperature in urban areas relative to their suburban or rural surroundings (Badugu et al. 2023). The surface urban heat island (SUHI) is a type of urban heat island developed as a result of difference in surface temperatures of urban and rural or suburban areas. Accordingly, a positive value means the presence of a SUHI whereas a negative value means the presence of surface urban freshness island (SUFI) (Alves et al. 2020).

For delineation of SUHI, a 5 km buffer around Bhubaneswar MC boundary is created (Fig. 11). This is the rural area from where the average rural surface temperature was obtained. The highest LST observed in the rural zone is 36.04 °C, 40.31 °C, and 40.28 °C

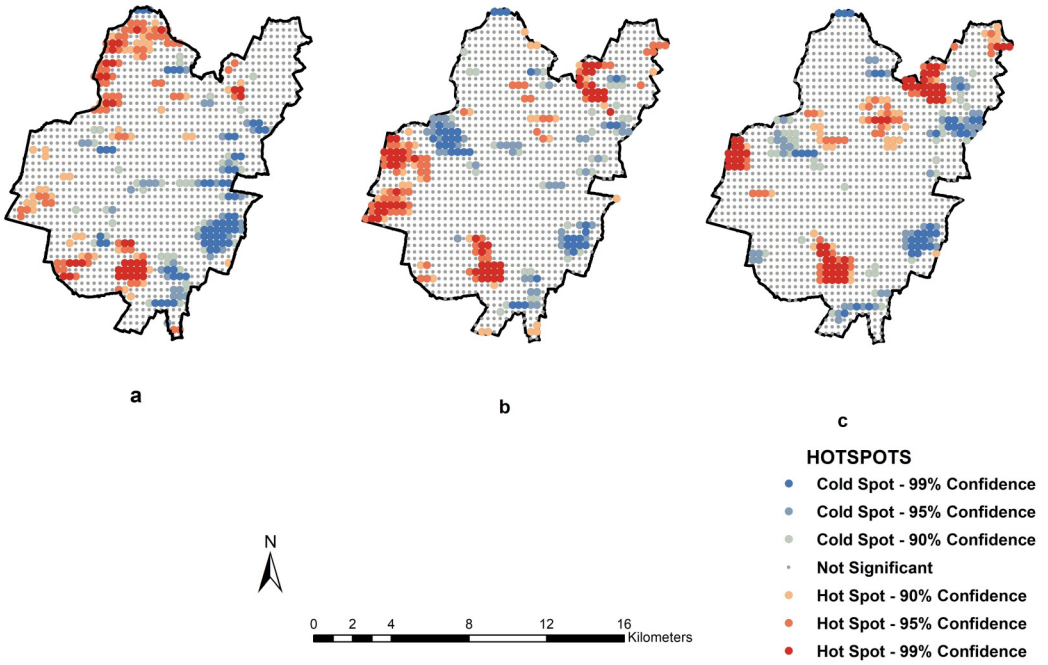


Fig. 10. Map showing hot spots in Bhubaneswar for the Year: a) 2001; b) 2011; c) 2021 using Getis-Ord Gi* tool

for 2001, 2011, and 2021 respectively which is greater than the highest LST within the city boundary. The lower LST of the same is 24.54 °C, 24.97 °C, and 25.95 °C for 2001, 2011, and 2021 respectively which are also lower than the lowest LST of the city. So, not only is the highest temperature of the surrounding region of the city higher than the inner city but the lowest is also lower than the inner city. The average rural surface temperature for 2001, 2011, and 2021 is 30.99 °C, 32.85 °C and 33. 52 °C respectively. The mean rural surface temperature is high in 2011 despite the presence of several green patches. This is due to the presence of a sand bed zone near Khuakhai river. The lower LST values for the

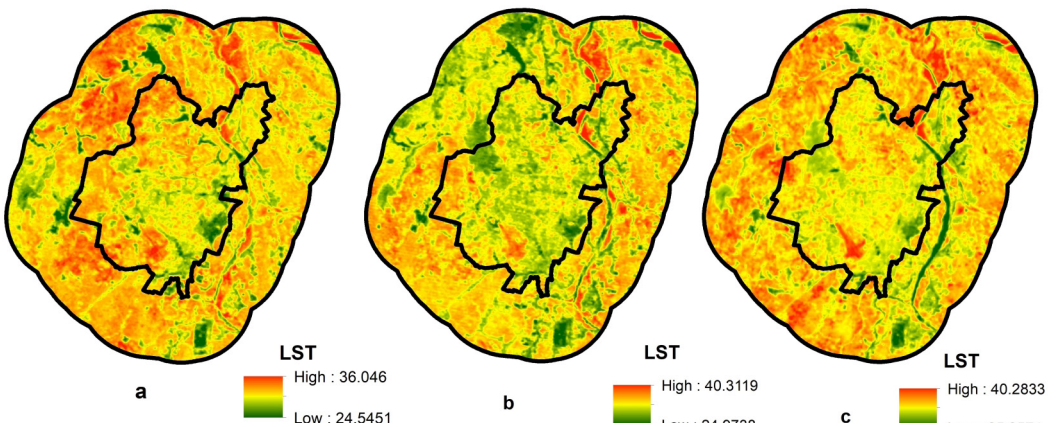


Fig. 11. Map showing LST of city with 5 km buffer zone from the city boundary for the years: a) 2001; b) 2011; c) 2021

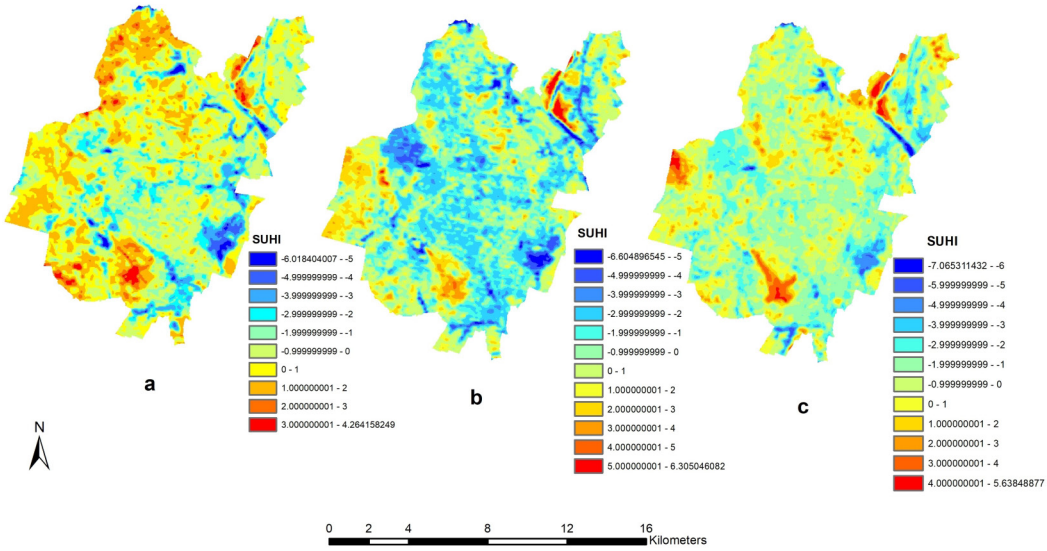


Fig. 12. Map showing SUHI and SUFI in Bhubaneswar of year: a) 2001; b) 2011; c) 2021

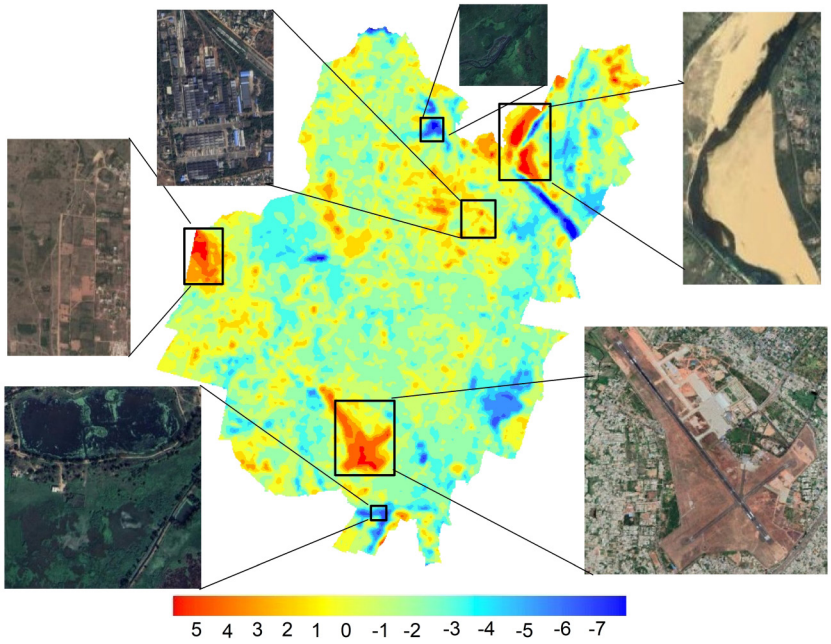


Fig. 13. Showing hot spots and cold spots of the city in 2021

year 2021 are observed over the water body in the rural area (Kuakhai river).

The NDBI and NDVI indices show maximum vegetation cover in the city in the year 2011 and minimum in 2001. Similarly, more patches representing SUFI are observed in the city in 2011 compared to more patches representing SUHI in 2001 (Fig. 12). Many patches representing SUHI in 2001 are converted to SUFI in 2021 but the SUHI patches in the airport and sand bed area have remained common throughout the years. In 2021, the new patches representing SUHI have developed (Fig. 13) in the north eastern

part (ward 10) (Bhubaneswar Municipal Corporation n.d.) of the city. This may be attributed to an increase in the residential and industrial areas like Mancheswar estate in these parts.

Dense vegetation and water bodies reduce the surface temperature of their surrounding areas whereas urban impervious surfaces and bare land do the opposite (Singh 2024; Karakous 2019; Dibaba 2023). The coastal city of Mumbai, known for its pleasant moderate temperature, has witnessed an increase of 5 ˚C in its mean LST in the last two decades (Waghchaure et al. 2022). Following the same trend, Bhubaneswar city has also experienced an overall rise of 4°C in average LST from 2001 to 2021. Notably, in the last decade, the LST increased by less than 1°C despite the high increase in built up area share of the city during this time. Impervious surfaces have been found to have a mean temperature 6 ˚C higher than the green spaces in Lucknow in 2016 and 8˚C higher than agricultural and barren land in Bengaluru in 2017 (Shukla – Jain 2021; Govind – Ramesh, 2019).

Contrary to the general trend established in previous studies (i.e. green areas have low LST), the greener central part of the city experienced a rise of 4˚C in LST — attributable to its surroundings having higher concrete proportion and thus, creating a doming effect on the overall region. Positive correlation between LST and NDBI and negative correlation between LST and NDVI were also observed i.e. the rise in built-up led to rise in temperature of the surrounding areas whereas increase in vegetation had a cooling effect on the surroundings. Previous works on LULC change dynamics and impacts on LST in Bhubaneshwar city have indicated a trend of decline in the vegetation cover, increase in built up and mean LST of the city, and differences in distributional pattern of LST in the city (core-periphery, scattered-concentrated, direction of high LST etc) and established a positive correlation of built up and LST (Das et al. 2022; Sarkar 2022; Samal et al. 2022). The assessment of LST, presence of SUHI and urban hot spots over the metro cities of Delhi and Mumbai (1991 to 2018) have also revealed that UHI gets intensified over the built-up surfaces and bare land where the value of LST is high whereas it becomes weak over the vegetation cover and water bodies (Swapan et al. 2022; Guha and Govil 2022). The assessment of SUHI in Bhubaneswar showed not only the highest LST values in the rural zone (buffer) being higher than the area within the city boundary but also the lowest LST values being lower than the inner city due to the influence of a river and sand bed zone in the rural area on the surface temperature.

For this study, Landsat imagery (30 m resolution) of a single season were used to estimate LST and SUHI via NDVI and NDBI spectral indices from 2001 to 2021. The limited image resolution and lack of field verification are a barrier in understanding the impact of vegetation quality and density on SUHI — which can help in creating better policies for tackling urban heat. The 5 km buffer zone for delineating rural area boundary may also be found lacking while covering the temperature differences since such a buffer usually comprises the rurban zone (or suburbs) and exhibits similar characteristics to that of the city, except the density. Nevertheless, this study has successfully identified urban hot and cold spots in the city where targeted action can be taken by the administration to improve the thermal profile and the microclimate of the area and thus, closed a significant gap in research carried out in Bhubaneshwar city. By taking into account the above shortcomings and adding population along with other weather/climatic parameters to the study, the potential improvement in its outcomes will help researchers in arriving at a more comprehensive result significant for urban sustainability and health.

## 4. Conclusion

Land use and land cover (LULC) fluctuations drastically alter the energy balance on the earth's surface, creating climate variations in a region (Zhi et al. 2020). As impervious surfaces replace vegetative cover on earth, LST rises, causing issues such as evapotranspiration rate changes, water modification, change in environment and energy balance, thereby, establishing the relationship of LST with built up expansion, construction materials, and vegetation in both rural and urban areas (Xiao 2007; Jiang 2010). The current study shows an increase in the built-up area of Bhubaneswar (2001-2021) from 19.05 sq. km to 46.98 sq. km (27.93 sq. km in total) and an increase in LST by 3.93℃ (maximum) and 1.55℃ (minimum). In Bhubaneswar, the LST values were higher in the north and north-east of the city (coinciding with the hotspots) where the airport, industries, and residential buildings are located. Low LST was observed over water bodies (Bindu sagar, Kuakhai river etc.) and vegetation patches (Bharatpur forest, Jaydev Bhatika etc.) that were also identified as cold spots. The heating effect of built up and cooling effect of vegetation on surrounding areas was ascertained as a positive correlation between LST and NDBI and a negative correlation between LST and NDVI was found. More noticeably, the overall vegetation cover of the city increased by 19.5 sq. km in two decades. This was due to several plantation drives and green space conservation efforts started by the Bhubaneswar Municipal Corporation (BMC) between 2005 to 2011 (Bhubaneswar Municipal Corporation n.d.). The increased vegetation patches were observed in educational institutions in the north-central part of the city. To conclude, this study has identified urban hot and cold spots in the city where targeted action can be taken by the administration to improve the thermal profile and the microclimate of the area. Thus, the outcome of the present research will contribute towards environmentally considerate urban planning and monitoring of the city, thereby, eventually improving the environmental sustainability of city and quality of life of the city dwellers. The analysis of LST will assist the government and urban planners in identifying pockets of heat stress. Therefore, it will lead to building of efficient management strategies and action plans like developing green spaces in and around cities with high average temperatures and ultimately, may lead to the development of Bhubaneswar as a sustainable smart city.

## 5. References

Abir, F.A. – Ahmmed, S. – Sarker, S.H. – Fahim, A.U. (2021): Thermal and ecological assessment based on land surface temperature and quantifying multivariate controlling factors in Bogura, Bangladesh. Heliyon. 7(9): e08012. https://doi.org/10.1016/j.heliyon.2021.e08012

Al-Ruzouq, R. – Naseeb, A. – Albakri, A.S. – Hammouri, N. – Zeiada, W. (2022): The relationship between air temperature and land surface temperature in a desert climate city. Remote Sensing Technologies and Applications in Urban Environments VII. SPIE Remote Sensing, Berlin, Germany, 2022. 12269: 64–70. https://doi.org/https://doi.org/10.1117/12.2636133

Alves, E. – Anjos, M. – Galvani, E. (2020): Surface Urban Heat Island in Middle City: Spatial and Temporal Characteristics. Urban Science. 4(4): 54. https://doi.org/10.3390/urbansci4040054

Anasuya, B. – Swain, D. – Vinoj, V. (2019): Rapid urbanization and associated impacts on land surface temperature changes over Bhubaneswar Urban District, India. Environmental Monitoring and Assessment. 191. https://doi.org/10.1007/s10661-019-7699-2

Badugu, A. – Arunab, K.S. – Mathew, A. – Sarwesh, P. (2023): Geodesy and Geodynamics Spatial and temporal analysis of urban heat island effect over Tiruchirappalli city using geospatial techniques. Geodesy and Geodynamics. 14(3): 275–291. https://doi.org/10.1016/j.geog.2022.10.004

Bhubaneswar Development Authority. (n.d.): https://www.bda.gov.in/bda/about-bda

Bhubaneswar Municipal Corporation. (n.d.): https://www.bmc.gov.in/about/zones-wards

Bhubaneswar Municipal Corporation. (n.d.): https://www.bmc.gov.in/services/plantation-services

Census India. (2011): https://www.censusindia2011.com/odisha/khordha/bhubaneswar-mcorp/bhubaneswar-m-corp-population.html

Chaudhuri, S. (2020): Evaluating the contribution of urban ecosystem services in regulating thermal comfort. Spatial Information Research. 29: 71-82. https://doi.org/10.1007/s41324-020-00336-8

City Development Plan Report. (2014): http://jnnurm.nic.in/wp-content/uploads/2010/12/bhubneshwar_Main_Report.pdf

Das, T. – Jana, A. – Mandal, B. – Sutradhar, A. (2022): Spatio-temporal pattern of land use and land cover and its effects on land surface temperature using remote sensing and GIS techniques: a case study of Bhubaneswar city, Eastern India (1991–2021). GeoJournal. 87: 765-795. https://doi.org/10.1007/s10708-021-10541-z

Deoli, V. (2020): Change Detection in Temperature using Remote Sensing and Satellite Data for Nainital District of Uttarakhand. International Journal of Current Microbiology and Applied Sciences. 9(11): 420–429. https://doi.org/10.20546/ijcmas.2020.911.051

Derdouri, A. – Wang, R. – Murayama, Y. – Osaragi, T. (2021): Understanding the links between LULC changes and SUHI in cities: Insights from two-decadal studies (2001–2020). Remote Sensing. 13(18). https://doi.org/10.3390/rs13183654

Dibaba, W.T. (2023): Urbanization-induced land use/land cover change and its impact on surface temperature and heat fluxes over two major cities in Western Ethiopia. Environmental Monitoring and Assessment. 195: 1083. https://doi.org/https://doi.org/10.1007/s10661-023-11698-5

Frost, J. (n.d.): How to Interpret R-squared in Regression Analysis. https://statisticsbyjim.com/regression/interpret-r-squared-regression/

Garg, R. (2022): Evaluating the impact of climate change on the urban environment using geospatial technologies in Bhubaneswar, India. The International Archives of the Photogrammetry, Remote Sensing and Spatial Information Sciences. XLVIII-4/W5-2022: 159-166.10.5194/isprs-archives-XLVIII-4-W5-2022-159-2022

Garg, R. D. (2023): Assessing the Cooling Effect of Blue-Green Spaces: Implications for Urban Heat Island Mitigation. Water 2023. 15(16): 2983. https://doi.org/https://doi.org/10.3390/w15162983

Govind, N. R. – Ramesh, H. (2019): The impact of spatiotemporal patterns of land use land cover and land surface temperature on an urban cool island: a case study of Bengaluru. Environmental monitoring and assessment. 191: 1–20. https://doi.org/https://doi.org/10.1007/s10661-019-7440-1

Guha, S. and Govil, H. (2022): Seasonal variability of LST-NDVI correlation on different land use/land cover using Landsat satellite sensor: a case study of Raipur City, India. Environ Dev Sustain 24, 8823–8839. https://doi.org/10.1007/s10668-021-01811-4

Halder, B. – Bandyopadhyay, J. – Khedher, K.M. – Fai, C.M. – Tangang, F. – Yaseen, Z.M. (2022): Delineation of urban expansion influences urban heat islands and natural environment using remote sensing and GIS-based in industrial area. Environmental Science and Pollution Research. 29(48): 73147–73170. https://doi.org/10.1007/s11356-022-20821-x

Jana, M. – Sar, N. (2016): Modeling of hotspot detection using cluster outlier analysis and Getis-Ord Gi* statistic of educational development in upper-primary level, India. Modeling Earth Systems and Environment. 2(2): 60. https://doi.org/10.1007/s40808-016-0122-x

Jiang, J. – Tian, G. (2010): Analysis of the impact of Land use/Land cover change on Land Surface Temperature with Remote Sensing. Procedia Environmental Sciences. 2(5):571–575. https://doi.org/10.1016/j.proenv.2010.10.062

Karakuş, C. B. (2019): The Impact of Land Use/Land Cover (LULC) Changes on Land Surface Temperature in Sivas City Center and Its Surroundings and Assessment of Urban Heat Island. Asia-Pacific Journal of Atmospheric Sciences. 55: 669–684. https://doi.org/10.1007/s13143-019-00109-w

Kshetri, T.B. (2018): NDVI, NDBI & NDWI Calculation Using Landsat 7,8. GeoWorld. 2: 32–34. https://www.researchgate.net/publication/327971920_NDVI_NDBI_NDWI_Calculation_Using_Landsat_7_8

Landsat 8 Data Users Handbook. (n.d.): https://www.usgs.gov/landsat-missions/landsat-8-data-users-handbook

Li, Z. – Duan, S.B. (2017): Land surface temperature. Comprehensive Remote Sensing. 5: 264–283. https://doi.org/10.1016/B978-0-12-409548-9.10375-6

Li, Z. –Tang B. –Wu, H. –Ren, H. –Yan, G. –Wan, Z. – Trigo, I. – Sobrino, J. (2013): Satellite-derived land surface temperature: Current status and

perspectives. Remote Sensing of Environment. 131: 14–37. https://doi.org/10.1016/j.rse.2012.12.008

Magotra, R. –Tyagi, A. –Kumar, M. –Shaw, M. –Bhatia, A. – Sharma, Y. (2020): Climate Adaptive Heat Action Plans for Vulnerable Poor A case study of Bhubaneshwar city, Odisha. International Conference on Sustainable Development, 2020. https://ic-sd.org/wp-content/uploads/2020/11/Rohit-Magotra_Climate-Adaptive-Heat-Action-Plans-for-Vulnerable-Poor-%D1%8FA-case-study-of-Bhubaneshwar-city-Odisha.pdf

Mathew, A. – Khandelwal, S. – Kaul, N. (2016): Spatial and Temporal Variations of Urban Heat Island Effect and the effect of Percentage Impervious Surface Area and Elevation on Land Surface Temperature: Study of Chandigarh City, India. Sustainable Cities and Society. 26: 264-277. https://doi.org/10.1016/j.scs.2016.06.018

Mathew, L. – Khare, A. – Khanna, B. – Shetty, B. – Pai, M. – Palanichamy, R.B. (WRI): (n.d.). An Advisory on Preparation. Deutsche Gesellschaft für Internationale Zusammenarbeit (GIZ) GmbH. Deutsche Gesellschaft für%0AInternationale Zusammenarbeit (GIZ) GmbH

Mcseveny, A. – Conway, R. – Wilkes, S. – Smith, M. (2014): Guideline for interpreting correlation coefficient. Pearson Australia, 2009. https://www.slideshare.net/phannithrupp/guideline-for-interpreting-correlation-coefficient

Najafzadeh, F. – Mohammadzadeh, A. – Ghorbanian, A. (2021): Spatial and Temporal Analysis of Surface Urban Heat Island and Thermal Comfort Using Landsat Satellite Images between 1989 and 2019: A Case Study in Tehran. Remote Sensing. 13(21): 4469. https://doi.org/10.3390/rs13214469

Nandini, G. –Vinoj, V. –Sethi, S. S. –Nayak, H. P. – Landu, K. –Swain, D. – Mohanty, U. C. (2022): A modelling study on quantifying the impact of urbanization and regional effects on the wintertime surface temperature over a rapidly - growing tropical city. Computational Urban Science. 2: 40. https://doi.org/10.1007/s43762-022-00067-6

Pritipadmaja. – Garg, R.D. (2022): Evaluating the Impact of Climate Change on The Urban Environment Using Geospatial Technologies in Bhubaneswar, India. The International Archives of the Photogrammetry, Remote Sensing and Spatial Information Sciences. XLVIII-4/W5-2022. 7th International Conference on Smart Data and Smart Cities (SDSC), Sydney, Australia, 19–21 October, 2022. https://doi.org/https://doi.org/10.5194/isprs-archives-XLVIII-4-W5-2022-159-2022

Samal, S. K. –Sa, B. S. – Sarkhel, P. (2022): Heat Stress & Its Negative Impact on the City and its Inhabitants : A Case Study of Bhubaneswar. International Journal for Research in Applied Science & Engineering Technology. 10(8): 848-856. https://doi.org/https://doi.org/10.22214/ijraset.2022.46293

Sarkar, A. A. (2022): Remote-Sensing-Based Analysis of Relationship Between Urban Heat Island and Land Use/Cover Type in Bhubaneswar Metropolitan Area, India. In: Jana, N.C., Singh, R.B. (eds) (2022): Climate, Environment and Disaster in Developing Countries. Advances in Geographical and Environmental Sciences. Springer, Singapore. 39-60. https://doi.org/https://doi.org/10.1007/978-981-16-6966-8_3

Sethi, S.S. – Vinoj, V. – Gogoi, P.P. – Landu, K. – Swain, D. (2022): Surface urban heat island (SUHI ) and its evolution over a rapidly growing tropical urban complex in Eastern India. SSRN Electronic Journal. http://dx.doi.org/10.2139/ssrn.4063144

Shahfahad, –Talukdar, S. –Rihan, M. –Hang, H.T. – Bhaskaran, S. – Rahman, A. (2022): Modelling urban heat island (UHI) and thermal field variation and their relationship with land use indices over Delhi and Mumbai metro cities. Environment, Development and Sustainability. 24(3): 3762–3790. https://doi.org/10.1007/s10668-021-01587-7,

Sharma, R. –Pradhan, L. –Kumari, M. – Bhattacharya, P. (2021): Assessing urban heat islands and thermal comfort in Noida City using geospatial technology. Urban Climate. 35: 100751. https://doi.org/10.1016/j.uclim.2020.100751

Shukla, A. –Jain, K. (2021): Analyzing the impact of changing landscape pattern and dynamics on land surface temperature of Lucknow city, India. Urban Forestry & Urban Greening. 58: 126877. https://doi.org/10.1016/j.ufug.2020.126877

Singh, K.K. (2024): Land surface temperature and thermal comfort in the cities of Punjab, India: assessment based on remote sensing data. Indian Journal of Science and Technology. 17(15): 1535-1544. https://doi.org/10.17485/IJST/v17i15.228

Swain, D. – Roberts, G.J. – Dash, J. – Lekshmi, K. – Vinoj, V. – Tripathy, S. (2017): Impact of Rapid Urbanization on the City of Bhubaneswar, India. Proceedings of the National Academy of Sciences, India, Section A: Physical Sciences. 87, 845–853. https://doi.org/10.1007/s40010-017-0453-7

Swapan, S. –Mohd, T. –Hoang, R. –Hang, T. – Bhaskaran, S. (2022): Modelling urban heat

island ( UHI ) and thermal field variation and their relationship with land use indices over Delhi and Mumbai metro cities. Environment, Development and Sustainability. 24(3): 3762–3790. https://doi.org/10.1007/s10668-021-01587-7

Tah, S. – Mukherjee, S. (2022): Seasonal distribution of urban heat using Landsat-8 multispectral data : A case study in Bhubaneshwar. Journal of Emerging Technologies and Innovative Research. 9(9): 323–332.

Turney, S. (2022): Pearson Correlation Coefficient (r) | Guide & Examples. https://www.scribbr.com/statistics/pearson-correlation-coefficient/

Vadapalli, P. (2023): How to Interpret R-squared in Regression Analysis? https://www.upgrad.com/blog/interpret-r-squared-in-regression-analysis/

Waghchaure, S. –Vijay, R. –Dey, J. –Thakre, C. (2022): Impact of Land-Use Dynamics on Land Surface Temperature in Mumbai City, India: A Geospatial Approach. Journal of Environmental Informatics Letters. 7(2): 69-79. https://doi.org/10.3808/jeil.202200080

Wang, F. – Qin, Z. – Song, C. – Tu, L. – Karnieli, A. – Zhao, S. (2015): An improved mono-window algorithm for land surface temperature retrieval from Landsat 8 thermal infrared sensor data. Remote Sensing. 7(4): 4268–4289. https://doi.org/10.3390/rs70404268

Wang, J. –Zhan, Q. – Guo, H. (2016): The Morphology, Dynamics and Potential Hotspots of Land Surface Temperature at a Local Scale in Urban Areas. Remote Sensing. 8(1). https://doi.org/ https://doi.org/10.3390/rs8010018

Xiao, H. –Weng, Q. (2007): The impact of land use and land cover changes on land surface temperature in a karst area of China. Journal of Environmental Management. 85(1): 245–257. https://doi.org/10.1016/j.jenvman.2006.07.016

Zhi, Y. –Shan, L. –Ke, L. – Yang, R. (2020): Analysis of Land Surface Temperature Driving Factors and Spatial Heterogeneity Research Based on Geographically Weighted Regression Model. Complexity. 2020: 2862917. https://doi.org/ https://doi.org/10.1155/2020/2862917